The Korean Journal of Rheology,
Vol. 10, No. 4, December 1998 pp. 202-216

<연구논문>

단섬유 보강 복합재료에서의 섬유배향의 수치모사를 위한 개선된 근사모델

정두환 · 권태헌
포항공과대학교 기계공학과
(1998년 10월 10일)

Improved Closure Approximation for Numerical Simulation of Fiber Orientation in Fiber-Reinforced Composite

D.H. Chung and T.H. Kwon
Department of Mechanical Engineering, Pohang University of Science and Technology,
San 31 Hyojadong Nam-ku, Pohang, Kyungbuk, 790-784, Korea
(Received October 10, 1998)

요 약

기존의 'Orthotropic' 근사모델의 개선된 형태인 ORW를 새로운 유동 자료를 이용하여 수치적으로 구하였다. 기존의 'Orthotropic' 근사모델인 ORF나 ORL은 특히 전단유동 하에서 상호작용상수 $C_I < 0.001$인 경우 비물리적 진동특성을 나타낸다. 물론 center-gated disk와 같은 비균일 유동하에서도 비물리적 진동특성을 나타내고 'Distribution Function Calculation'과 비교하여 배향 상태를 낮게 예측한다. 이런 현상들은 바로 least-square 최적화 시 사용된 유동 자료에 기인한 것을 알 수 있었다. 작은 상호작용계수의 균일 유동 자료를 이용하여 최적화를 한 ORW의 경우 비물리적 진동특성도 나타나지 않았고 균일 및 비균일 유동하에서 모두 정성적으로 잘 일치함을 확인할 수 있었다. 최적화 시 사용된 함수의 선택은 근사모델을 발전시키는데 그다지 영향을 미치지 못하였다. 하지만, 모든 배향 텐서의 eigenvalue들을 고려하면 보다 정량적으로 발전시킬 수 있지만 이들의 함수모양 선택은 중요하고 어려운 문제다. 비교를 위하여 ORW와 다른 여러 가지 근사모델을 이용하여 Film-gated strip과 Center-gated disk에 대한 연계효과 및 평면 속도구배를 포함한 사출성형 충전공정의 수치모사를 수행하였다. ORW가 'Distribution Function Calculation' 과 비교하여 정량적으로도 거의 비슷한 결과를 예측함을 보여주지만 실제 실험자료와 비교하였을 때 약간의 차이가 있음을 확인하였다. 따라서 좀 더 정확히 섬유의 배향도를 예측하기 위해서는 섬유들의 상호작용을 나타내는 항의 모델링의 변화가 요구된다.

Abstract— Improved version of previous 'Orthotropic' closure approximation, termed 'ORW' has been numerically developed using new homogeneous flow data. Previous 'Orthotropic' closure approximation, i.e., ORF or ORL showed non-physical oscillation for interaction coefficient $C_I < 0.001$ at simple shear flow. It also shows non-physcial oscillation and under-prediction compared with 'Distribution Function Calculation' at non-homogeneous flow of center-gated disk. These phenomena are mainly due to the flow data of 'Distribution Function Calculation' which were used for least-square optimization. ORW obtained by fitting flow data of low interaction coefficient does not show non-physical oscillation and results in reasonably good behaviors at non-homogeneous flows as well as homogeneous flows. Fitting function forms have not been found to improve overall behaviors. It has been found that considering all the eigenvalues of orientation tensor (including the third eigenvalues) might end up with a better closure approximation than just considering the first and second eigenvalues. It is, however, very important and yet difficult to select appropriate function forms of eigenvalues. Numerical simulation including coupling and in-plane velocity gradient effects were performed for injection mold filling process with a film-gated strip and a center-gated disk using ORW and various other closure approximations for comparisons. Although ORW is in excellent agreement with 'Distribution Function Calculation', the predicted results seem to have consistent error in comparison with experimental data. The diffusivity term with constant interaction coefficient might have to be further investigated in order to accurately describe orientation states.

Keywords: Fiber-Reinforced Composites, Homogenesous and Non-Homogeneous Flow, DFC, ORF, ORW, Closure Approximation, Eigenvalues, Coupling and In-Plane Velocity Gradient Effects, Interaction Coefficient, Diffusivity

1. Introduction

Injection molding of short-fiber-reinforced plastics is one of the most widely used polymer processing methods for the structural plastics parts. The thermo-mechanical properties of short-fiber-reinforced injection molded parts depend significantly on fiber orientation state. The prediction of fiber orientation and thermo-mechanical properties is important for good structural design. Prediction of thermo-mechanical properties with fiber orientation has been well

developed[1]. However, prediction of fiber orientation state is very difficult and even the physical mechanisms of fiber orientation during filling process have not been fully understood yet. The flow during a mold filling process plays an important role in forming a flow-induced fiber orientation, while the flow field is in turn affected by the fiber orientation. Therefore, including coupling effect between fiber orientation and flow field is important and Chung and Kwon[2,3] incorporated the Dinh-Armstrong model[4], including an additional stress due to the existence of fibers and in-plane stretching stress terms into the Hele-Shaw equation, to result in a new pressure equation governing the injection molding filling process.

The motion of a single rigid ellipsoidal particle immersed in a viscous Newtonian liquid was solved by Jeffery[5]. His evolution equation is valid for dilute suspensions and becomes the starting point of almost all the constitutive modelling. However, he did not take into account particle-particle interactions. Folgar and Tucker[6] developed an evolution equation for concentrated fiber suspensions, where the fiber-fiber interactions are taken into account by adding a diffusion term to Jeffery's equation. Advani and Tucker[7] adopted tensor representation to describe fiber orientation state using probability distribution function. It is very general and concise description. However, it is necessary to make some sort of closure approximation to obtain a closed set of equations. Therefore, several closure approximations have been suggested. So-called Hybrid closure approximation proposed by Advani and Tucker is one of them. Bay and Tucker[8] examined the fiber orientation in simple injection molding(a film-gated strip and a center-gated disk) and predicted the outer skin layer by including the effects of fountain flow and heat transfer. They insisted that the major source of error between the predicted and experimental results is the closure approximation used in the evolution equation for the orientation tensor.

Several closure approximations have been introduced by many researchers. Linear closure approximation(LIN) was first introduced by Hand[9] requiring tensorial expression to be symmetric with respect to any pair of indices and to meet the normalization condition. It is exact for an isotropic (random) distribution. Quadratic closure approximation(QUA) [10-12] was formed by taking the dyadic product of the second-order tensor with itself. It is exact for perfectly aligned fibers. Hinch and Leal[13] derived a number of different closure approximations. They did not give explicit formulas for a_{ijkl}. Rather, they derived approximations for the product $a_{ijkl}\dot{\gamma}_{kl}$. Their closure approximations, however, do not provide accurate solutions for all the flows and show non-physical oscillations in some cases. Advani and Tucker[7,14] formed Hybrid closure approximation(HYB) by mixing the quadratic and linear forms according to some scalar measure of orientation. It is still generally used, but it over-predicts orientation states for every flow field. Verleye and Dupret[15] developed Natural closure approximation(NAT) which assumes a general form for a_{ijkl} in terms of a_{ij}. They adopted polynomial expansions of principal invariants for unknown coefficients, and matched with analytical solution without considering fiber-fiber interaction using a least square procedure. It showed good transient behavior but results in a little over-prediction of steady state orientation field. Cintra and Tucker[16] developed Orthotropic closure approximation(ORF, ORL) by assuming that the principal directions of 4^{th} order tensor match with 2^{nd} order tensor and that 4^{th} order principal values are functions of the eigenvalues of 2^{nd} order tensor. Orthotropic closure approximation is almost the same as Natural closure approximation in a sense that assuming a functional form for 4^{th} order tensor and fitting with exact values. ORF(or ORL) shows better behavior than previous closure approximations but suffers from non-physical oscillation at low value of interaction coefficient. It will be shown later that it is mainly due to flow data used for least-square optimization. Orthotropic closure approximation is very sensitive to flow data and interaction coefficients used for least-square optimization.

Present research is aimed at improving previous Orthotropic closure approximation which does not show non-physical oscillation in both homogeneous and non-homogeneous flow fields even at low value of interaction coefficients. We call exact orientation description using 'Distribution Function Calculation' DFC. Good closure approximations are supposed to match well what DFC predicts. In this regard, we developed closure approximation such that it predicts values which are in good agreement with DFC results. We adopted isothermal Newtonian radial diverging flow(center-gated disk flow) as a bench mark test problem to check the performance of any closure approximations, because it is a non-homogeneous flow having both shear flow and elongational flow together compared with homogeneous flow fields(i.e., simple shear flow, elongational flow). The improved version of previous Orthotropic closure approximation we obtained is called ORW, which can be applied to a wide range of the C_I values.

Numerical simulations are extensively performed which take into account 'coupling efffects between flow and orientation' and in-plane velocity gradients as well as usual shear effects. Simulated data are compared with experimental data of Bay and Tucker[8] for a film-gated strip and a center-gated disk.

2. Theories

2.1. Fiber Orientation

There are several different approaches describing the fiber orientation state in short-fiber-reinforced injection molding process, but because of the computational efficiency, orientation tensors are mainly used for a more compact representation of the orientation state of fibers.

The orientation state of a group of fibers can be described by a probability distribution function $\psi(p)$, defined so that the probability of a fiber being oriented within an angular range dp of the direction p is equal to $\psi(p)dp$. The second and fourth order tensor are defined as follows:

$$a_{ij} = \int p_i p_j \psi(p) dp$$

$$a_{ijkl} = \int p_i p_j p_k p_l \psi(p) dp$$

Groups of fibers may be modelled by solving for the probability distribution function $\psi(p)$. Combining the following conservation equation(Eq. (1)) for ψ in p space and the fiber angular velocity equation(Eq. (2)) leads to governing equation for $\psi(p)$.

$$\frac{D\psi}{Dt} = -\frac{\partial}{\partial p} \cdot (\psi \dot{p}) \tag{1}$$

$$\dot{p}_i = -\frac{1}{2}\omega_{ij}p_j + \frac{1}{2}\lambda(\dot{\gamma}_{ij}p_j - \dot{\gamma}_{kl}p_k p_l p_i) - \frac{D_r}{\psi}\frac{\partial \psi}{\partial p_i} \tag{2}$$

The evolution equation for the second-order orientation tensor a_{ij} can be expressed as follows:

$$\frac{Da_{ij}}{Dt} = -\frac{1}{2}(\omega_{ik}a_{kj} - a_{ik}w_{kj}) + \frac{1}{2}\lambda(\dot{\gamma}_{ik}a_{kj} + a_{ik}\dot{\gamma}_{kj} - 2\dot{\gamma}_{kl}a_{ijkl}) + 2D_r(\delta_{ij} - 3a_{ij}) \tag{3}$$

where $w_{ij}=u_{j,i}-u_{i,j}$ is the vorticity tensor, $\dot{\gamma}_{ij}=u_{j,i}+u_{i,j}$ the rate of deformation tensor, and δ_{ij} the identity tensor. $\lambda = \frac{((L/D)^2-1)}{((L/D)^2+1)}$ is a parameter related to the aspect ratio of the fiber L/D.

The rotary diffusivity D_r is used to model fiber-fiber interaction in concentrated suspensions. Folgar and Tucker [6] suggested that D_r could be modelled by $C_I\dot{\gamma}$, where an interaction coefficient C_I is an empirical coefficient that must be determined by comparing predictions with experiments, $\dot{\gamma}$ being the generalized shear rate defined by $\dot{\gamma} = \sqrt{\dot{\gamma}_{ij}\dot{\gamma}_{ji}/2}$.

2.2. Mold Filling Flow

The anisotropic constitutive equation, including an additional stress due to the existence of fibers, should be introduced for the coupled analysis of the injection molding filling flow and the fiber orientation. Using Batchelor's cell model[17], Dinh and Armstrong[4] developed a rheological equation of state for semi-concentrated fiber suspensions where the average spacing h between neighboring fibers is greater than its diameter D, but less than its length L. The constitutive equation of this model can be described as follows:

$$\tau_{ij} = \eta(u_{i,j} + u_{j,i}) + \eta N u_{k,l} a_{ijkl} \tag{4}$$

where the dimensionless parameter N representing the anisotropic contributions from the fibers, called the particle number[18] is given by

$$N = \frac{\pi n L^3}{6\ln(2h/D)} \tag{5}$$

with

$$h = \begin{cases} (nL^2)^{-1} & \text{for random orientation} \\ (nL)^{-1/2} & \text{for aligned orientation} \end{cases}$$

In the simulation, it is assumed that the average distance from a given fiber to its nearest neighbors h is linear in terms of the scalar measure of orientation f, which varies from zero to unity according to the orientation state of fibers. When the number of fibers per unit volume n is greater than $1/(DL^2)$, the average distance between fibers is assumed to be the same as for the aligned orientation state independent of the orientation state. Therefore, in this study, h is described as

$$h = (1-f)h_{random} + fh_{aligned} \quad \text{for} \quad \frac{\pi}{4}\left(\frac{D}{L}\right)^2 < v_f < \frac{\pi}{4}\left(\frac{D}{L}\right)$$

$$h = h_{aligned} \quad \text{for} \quad \frac{\pi}{4}\left(\frac{D}{L}\right) \le v_f < \frac{\pi}{4} \tag{6}$$

$$f = 1 - 27\det[a_{ij}] \tag{7}$$

The injection mold filling flow for fiber suspensions including coupling effects between flow and fiber orientation with in-plane velocity gradient effects is governed by the following equations:

pressure equation

$$\frac{\partial}{\partial x}\left[(S-S^x)\frac{\partial P}{\partial x}-S^{xy}\frac{\partial P}{\partial y}-F^x\right]+\frac{\partial}{\partial y}\left[(S-S^y)\frac{\partial P}{\partial y}-S^{xy}\frac{\partial P}{\partial x}-F^y\right]=0 \quad (8)$$

where

$$N^x=\frac{Na_{3113}(1+Na_{3223})-N^2a_{2123}a_{3213}}{(1+Na_{3113})(1+Na_{3223})-N^2a_{3123}a_{3213}}$$

$$N^y=\frac{Na_{3223}(1+Na_{3113})-N^2a_{3123}a_{3213}}{(1+Na_{3113})(1+Na_{3223})-N^2a_{3123}a_{3213}}$$

$$N^{xy}=\frac{Na_{3123}}{(1+Na_{3113})(1+Na_{3223})-N^2a_{3123}a_{3213}}$$

$$f^x=\eta Nu_{\alpha,\beta}a_{31\alpha\beta}|_z+\int_0^z(tea_{xx,x}+\tau_{yx,y})d\tilde{z}$$

$$f^y=\eta Nu_{\alpha,\beta}a_{32\alpha\beta}|_z+\int_0^z(tea_{zy,z}+tea_{yy,y})d\tilde{z}$$

$$S=\int_0^b\frac{\tilde{z}^2}{\eta}d\tilde{z}\qquad S^x=\int_0^bN^x\frac{\tilde{z}^2}{\eta}d\tilde{z}\qquad S^y=\int_0^bN^y\frac{\tilde{z}^2}{\eta}d\tilde{z}$$

$$S^{xy}=\int_0^bN^{xy}\frac{\tilde{z}^2}{\eta}d\tilde{z}\qquad F^x=\int_0^b\frac{\tilde{z}}{\eta}[(1-N^x)f^x-N^{xy}f^y]d\tilde{z}$$

$$F^y=\int_0^b\frac{\tilde{z}}{\eta}[(1-N^y)f^y-N^{xy}f^x]d\tilde{z}$$

Local Cartesian coordinates are chosen such that x and y coordinates are lying on the surface of thin cavity thickness molds, z being the gap-wise coordinate.

Boundary conditions on the pressure equation are P=0 on the moving flow front $\bar{u}\cdot n_x+\bar{v}\cdot n_y=0$ on the impermeable boundaries.

Pressure equation for fiber suspensions includes the extra terms(s^x, s^y, s^{xy}, F^x, F^y) due to the additional stress of fibers, and F^x, F^y represents the x and y directional in-plane velocity gradient effect. Refer to[2,3] for the detailed informations.

A modified Cross model has been employed for the viscosity of the thermoplastic medium:

$$\eta(\dot{\gamma},T)=\frac{\eta_0}{1+C(\eta_0\dot{\gamma})^{1-m}},\qquad \eta_0=B\exp\left(\frac{T_b}{T}\right) \quad (9)$$

where m,B,C and T_b are constants for a given material.

energy equation

$$\rho C_p\left(\frac{\partial T}{\partial t}+u\frac{\partial T}{\partial x}+v\frac{\partial T}{\partial y}\right)=k\frac{\partial^2T}{\partial z^2}+\eta\dot{\gamma}^2 \quad (10)$$

Appropriate boundary conditions in the z-direction are the uniform temperature at the mold wall z=b and the symmetric condition at the mid-plane z=0

A detailed implementation of numerical analysis is described in Ref. 2 and 3. In this work, fountain flow and the fiber-wall interaction have been neglected.

2.3. Closure Approximation

A closure approximation is inherently required to obtain a closed set of evolution equations for orientation tensors, i.e., a suitable closure approximation for the fourth-order tensor a_{ijkl} must be introduced to solve Eq. (3). in terms of a_{ij} and δ_{ij}.

2.3.1. Hybrid closure approximation(HYB)

Hybrid closure approximation $\bar{a}_{ijkl}$(HYB) which is generally used in many software packages describes as follows:

$$\bar{a}_{ijkl}=(1-f)\hat{a}_{ijkl}+f\tilde{a}_{ijkl} \quad (11)$$

f: a scalar measure of orientation as in Eq. (7)

where $\hat{a}_{ijkl}=-\frac{1}{35}\left(\delta_{ij}\delta_{kl}+\delta_{ik}\delta_{jl}+\delta_{il}\delta_{jk}\right)+\frac{1}{7}\left(a_{ij}\delta_{kl}+a_{ik}\delta_{jl}+a_{il}\delta_{jk}+a_{kl}\delta_{ij}+a_{jl}\delta_{ik}+a_{jk}\delta_{il}\right)$ represents the linear closure

while $\tilde{a}_{ijkl}=a_{ij}a_{kl}$ stands for the quadratic closure.

2.3.2 Orthotropic closure approximation(ORF, ORL)

A short summary of Orthotropic closure approximation is as follows: Basic assumptions are that the principal axes of 4th order tensor match those of 2nd order tensor and principal values of 4th order tensor are functions of those of 2nd order tensor. With full symmetry conditions and normalization conditions, there are only three independent components of principal values of 4th order tensor. So, it reduces to the task of forming a closure approximation by choosing just three scalar functions of two unknowns each. That is, one must choose

$$\bar{A}_{11}=f_{11}(a_1,a_2)$$
$$\bar{A}_{22}=f_{22}(a_1,a_2)$$
$$\bar{A}_{33}=f_{33}(a_1,a_2) \quad (12)$$

where $\bar{A}_{11}$, $\bar{A}_{22}$, $\bar{A}_{33}$ are independent 4th order principal values and a_1, a_2 are two largest eigenvalues of 2nd order tensor.

The closure is chosen to match the fourth-order tensor values that are generated by the dynamics of fiber orientation(Eqs. (1)-(2)). The steps in the calculation are as follows:

(a) Select a set of flow fields that will generate a wide variety of orientation states.

(b) For each flow field: (i) Select an initial condition

for $\psi(p)$ and find $\psi(p, t)$. (ii) Select representative time steps, and at each time evaluate the exact orientation tensors a_{ij} and a_{ijkl}. (iii) At each time calculate the eigenvalues and eigenvectors of a_{ij}, and transform the fourth-order tensor into the principal axes, finding the values of $\bar{A}_{mm}$.

(c) For each independent component of $\bar{A}_{mm}$, collect all computed values as a function of the corresponding values of a_1 and a_2 based on Eq. (12). Use a least-squares-type fitting procedure to generate an approximation for each $\bar{A}_{mm}$ that best fits the data.

The flow fields Cintra and Tucker[16] selected for ORF are as follows with G and E representing shear rate and elongation rate, respectively.

① Simple shear, $u=Gx_2$, $v=w=0$

② Two shearing/stretching flows, which superimpose a simple shear flow in the 1-2 plane with uniaxial elongation in the 3 direction, $u=-Ex_1+Gx_2$, $v=-Ex_2$, $w=2Ex_3$. For case A with G/E=20 the shearing and stretching are nearly balanced, while for case B with G/E=1 the stretching is dominant.

③ Uniaxial elongation, $u=2Ex_1$, $v=-Ex_2$, $w=-Ex_3$.

④ Biaxial elongation, $u=Ex_1$, $v=Ex_2$, $w=2Ex_3$.

The least-square type fitting procedure can be expressed as follows: Following χ^2 value must be minimized.

$$\chi^2 = \sum_{i=1}^{NDATA} \sum_{m=1}^{6} \left\{ \bar{A}_{mm}^{i} - \bar{A}_{mm}^{i\,closure} \right\}^2 \qquad (13)$$

where $\bar{A}_{mm}^{i}$ represents the i^{th} data point obtained from the distribution function results, and $\bar{A}_{mm}^{i\,closure}$ is the corresponding value generated by the closure approximation. For the closure values complete second-order polynomials in a_1 and a_2 are adopted:

$$\bar{A}_{mm}^{closure} = C_m^1 + C_m^2 a_1 + C_m^3 [a_1]^2 + C_m^4 a_2 + C_m^5 [a_2]^2 + C_m^6 a_1 a_2 \qquad (14)$$

m=1, ···, 6: no sum on m.

It is final task to get 36 coefficients C_m^k. Detailed explanations about ORF closure approximation are described in Ref. 16.

Since Cintra and Tucker found that behavior of ORF in simple shear flow suffers from non-physical oscillation when C_I is less than 0.001, they have come up with ORL by introducing different flow data of different C_I with a hope to eliminate the non-physical oscillation. ORL implements the same flow data as ORF except replacing simple shear data of C_I=0.01 by that of C_I=0.001 and omitting data of shear/stretch flow B. It turns out that ORL did successfully eliminate the non-physical oscillation in simple shear flow for C_I=0.001[16]. For simple shear case with C_I=0.001, Fig. 1 clearly shows that ORL does not show non-physical oscillation as opposed to ORF, but slightly over-predicting flow directional orientation in comparison with DFC. Unfortunately, however, ORL failed in eliminating the non-physical oscillation in case of radial diverging flow for C_I=0.001, as will be described in this paper.

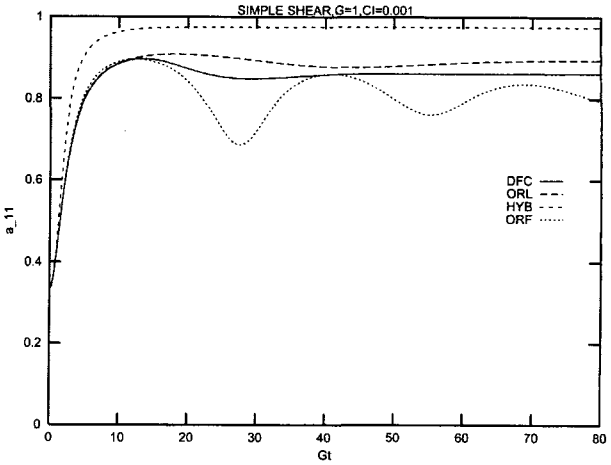

Fig. 1. DFC, ORL, HYB, ORF in simple shear flow for C_I=0.001.

2.3.3. Improvement of Orthotropic closure approximation (ORW)

In this work, an improvement of previous Orthotropic closure approximations(ORF and ORL) has been made to overcome such a non-physical oscillation in radial diverging flow for low values of C_I.

Our improved versions of the above ORF and ORL closure approximation, 'Test1' and ORW are summarized as follows:

ORF type closure approximation is quite dependent upon which flow data with corresponding interaction coefficients are used for fitting. Our extensive numerical experiments indicated that functional forms for $\bar{A}_{mm}^{closure}$ did not significantly influence overall behaviors unless third eigenvalues a_3 are included. Therefore, we focused our attempt on choosing optimal flow data which could cover all the orientation states of fibers. We have also chosen λ=1, $0.0001 < C_I < 0.01$ as representative values for fiber orientation modelling in injection-molded composites. For the flow fields, in addition to the five flow data described above, we selected the following cases to be included in the fitting:

⑤ Two shear/planar elongation, which superimpose 1-3 plane simple shear with 1-2 plane planar elongation. u=

$-Ex_1+Gx_3$, $v=Ex_2$, $w=0$. For case A with G/E=10, shearing and planar elongation are nearly balanced, while for case B with G/E=1, planar elongation is dominant.

⑥ Balanced shear/biaxial elongation, which superimpose 1-3 plane simple shear with biaxial elongation. $u=Ex_1+Gx_3$, $v=Ex_2$, $w=-2Ex_3$. $2\leq G/E\leq 5$ were used.

'Test1' and ORW adopted same flow fields (①~⑥) but 'Test1' implements with $C_I\geq 0.001$ while ORW implements with $C_I\geq 0.0001$. Detailed informations on 36 new coefficients of ORW are presented in the Appendix.

Above flow fields (①~⑥) cover all the orientation states of fibers throughout the eigenvalue domain and include extreme cases(uniaxial and biaxial elongation) as shown in Fig. 2. It is important that the shear/planar elongational flow (⑤) together with the shear/stretching balanced flow fields (②) be included in fitting data, so that it is possible that ORW closure approximation is applicable to non-homogeneous flow fields(in particular, radial diverging flow) as well as homogeneous flow fields.

It is very interesting to note that including the third eigenvalue(a_3) explicitly into Eq. (12) in addition to the first and the second eigenvalues(a_1, a_2) is found to make the orientation state very unstable. However, neglecting effects of a_3 make it impossible to accurately catch the transient states of orientation, especially at the simple shear flow where out-of-plane orientation components play an important role. Although it would be general to include a_3 in the formulation, more rigorous function forms for eigenvalues are required to develop more exact closure approximation, which remains to be resolved in the future work. This necessitates more theoretical and physical bases for fiber orientaton dynamics.

We have also attempted to replace the independent variables a_1 and a_2 in Eq. (14) with second and third invariants of a_{ij}(**II**, **III**), but failed in obtaining converged values of C_m^k in the fitting process with satisfaction. With such an extensive effort to improve the Orthotropic closure approximations, we present only the result with a_1 and a_2 as independent variables. Function forms for the closure approximation presented below are the same as those of ORF or ORL. So the only difference between ORF, ORL and 'Test1' or ORW closure approximations is the values of 36 coefficients c_m^k in Eq. (14). First, we will show several features of our new closure approximations in comparison with DFC values in several homogeneous (simple shear flow, shear/stretch flow) and non-homogeneous (isothermal Newtonian radial diverging flow) flow fields. Also, we have performed coupled analysis of mold filling and fiber orientation including in-plane velocity gradient effects for a film-gated-strip and a center-gated disk case and compared with the experimental data of Bay and Tucker[8].

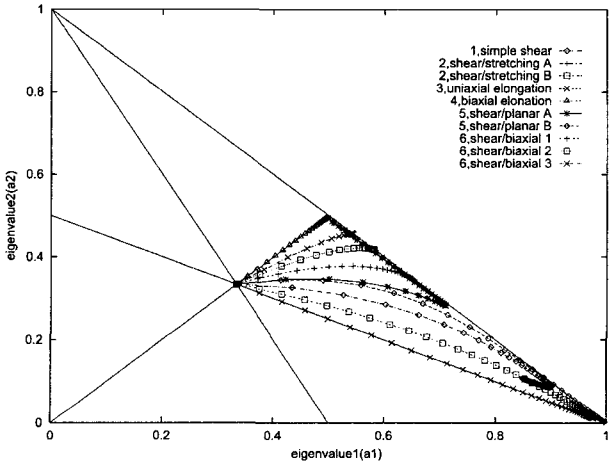

Fig. 2. Typical fitting data of flow field for ORW closure approximation.

3. Numerical Analysis Results and Discussion

3.1. Comparisons of Closure Approximations with DFC

We will discuss performance of HYB(Hybrid closure approximation), ORF or ORL(Orthoropic closure approximation) and the new closure approximations('Test1' and ORW) and compare their features in several flow fields, especially at isothermal, Newtonian radial diverging flow fields of a center-gated disk filling.

For isothermal, Newtonian radial diverging flow fields in a center-gated disk filling, the velocity field is

$$u_r=\frac{3Q}{8\pi b}\left(1-\frac{z^2}{b^2}\right),\quad u\theta=u_z=0 \tag{15}$$

If one adopts a local Cartesian coordinate system in which the(1, 2, 3) axes correspond to(r, θ, z), the velocity gradients can be obtained from Eq. (15) as

$$\frac{\partial u_i}{\partial x_j}=\frac{3Q}{8\pi b}\begin{bmatrix}-\frac{1}{r}\left(1-\frac{z^2}{b^2}\right) & 0 & -\frac{2}{b}\left(\frac{z}{b}\right)\\ 0 & \frac{1}{r}\left(1-\frac{z^2}{b^2}\right) & 0\\ 0 & 0 & 0\end{bmatrix} \tag{16}$$

The flow is in the 1-direction with stretching in the 2-direction, and shearing across the 3-direction. The ratio between the shear and elongation rates varies continuously across the gap and along the radial locations, which

makes this non-homogeneous flow an ideal bench mark test case of various closure approximations.

Shown in Fig. 3 are a_{11} components as a function of normalized radial location(r/b) at several gap-wise thickness positions(z/b) for the cases of DFC, ORF, ORL and HYB with C_I=0.001. HYB closure approximation(Fig. 3b) shows over-prediction in comparison with DFC(Fig. 3a). Both ORF and ORL indicate clearly non-physical oscillation in contrast to DFC for $C_I \leq 0.001$. Even if ORL does not suffer from non-physical oscillation in simple shear flow, as indicated in Fig. 1, the non-physical oscillation in the case of the isothermal Newtonian radial diverging flow (Fig. 3d) is certainly dissapointing and thus is regarded as a critical defect of ORL which was originally proposed to be applied to a small value of C_I=0.001. In contrast, as shown in Fig. 4, 'Test 1' and ORW do not show any oscillation and seem to be in much better agreement with DFC than the cases of ORF or ORL for C_I=0.001. 'Test 1' slightly under-predicts flow directional orientation components compared with DFC at core and transition layers but pretty much well agrees with DFC at shell layer. On the other hands, ORW over-predicts flow directional orientation components compared with DFC at shell layer, but pretty much well matches with DFC at core and transition layer.

When C_I is further decreased up to C_I=0.0002, ORF(or ORL) and 'Test 1' show oscillation behavior, but ORW matches with DFC qualitatively well as indicated in Fig. 5. For a relatively large value of C_I=0.01, ORL, 'Test 1' and ORW do not show any difference between them compared with DFC, but ORF shows slightly better behavior as shown in Fig. 6.

Therefore, one can conclude that ORW predicts the fiber behaviors quite well over the wide range of C_I, i.e., for $C_I > 0$.

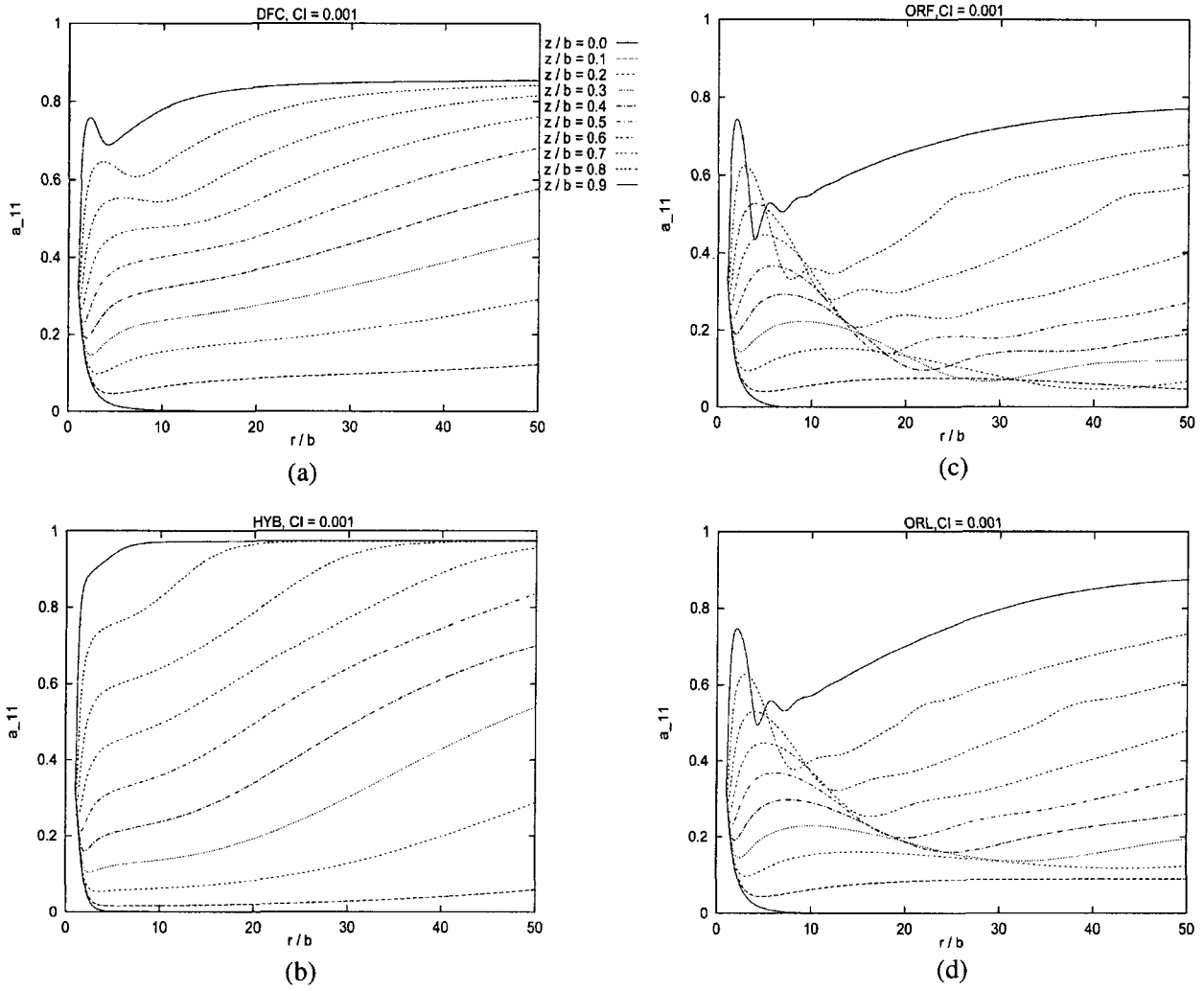

Fig. 3. a_{11} component in isothermal Newtonian radial diverging flow as a function of radial location (r/b) at several thickness positions (z/b) for various closure approximations with C_I=0.001: (a) DFC, (b) HYB, (c) ORF and (d) ORL.

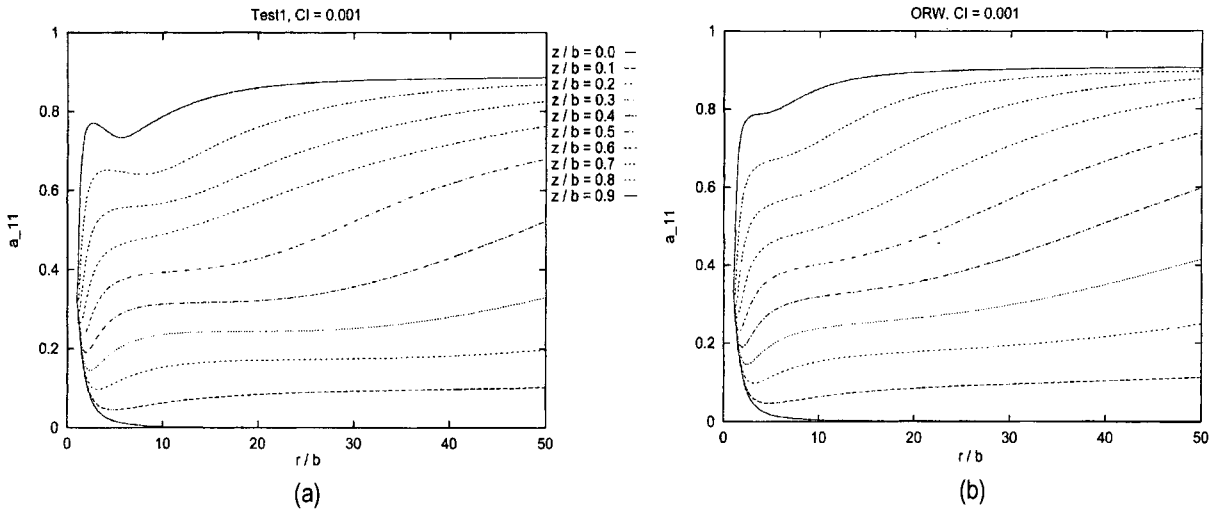

Fig. 4. a_{11} component in isothermal Newtonian radial diverging flow as a function of radial location (r/b) at several thickness positions (z/b) for various 'Test1' and ORW with C_I=0.001: (a) 'Test1' and (b) ORW.

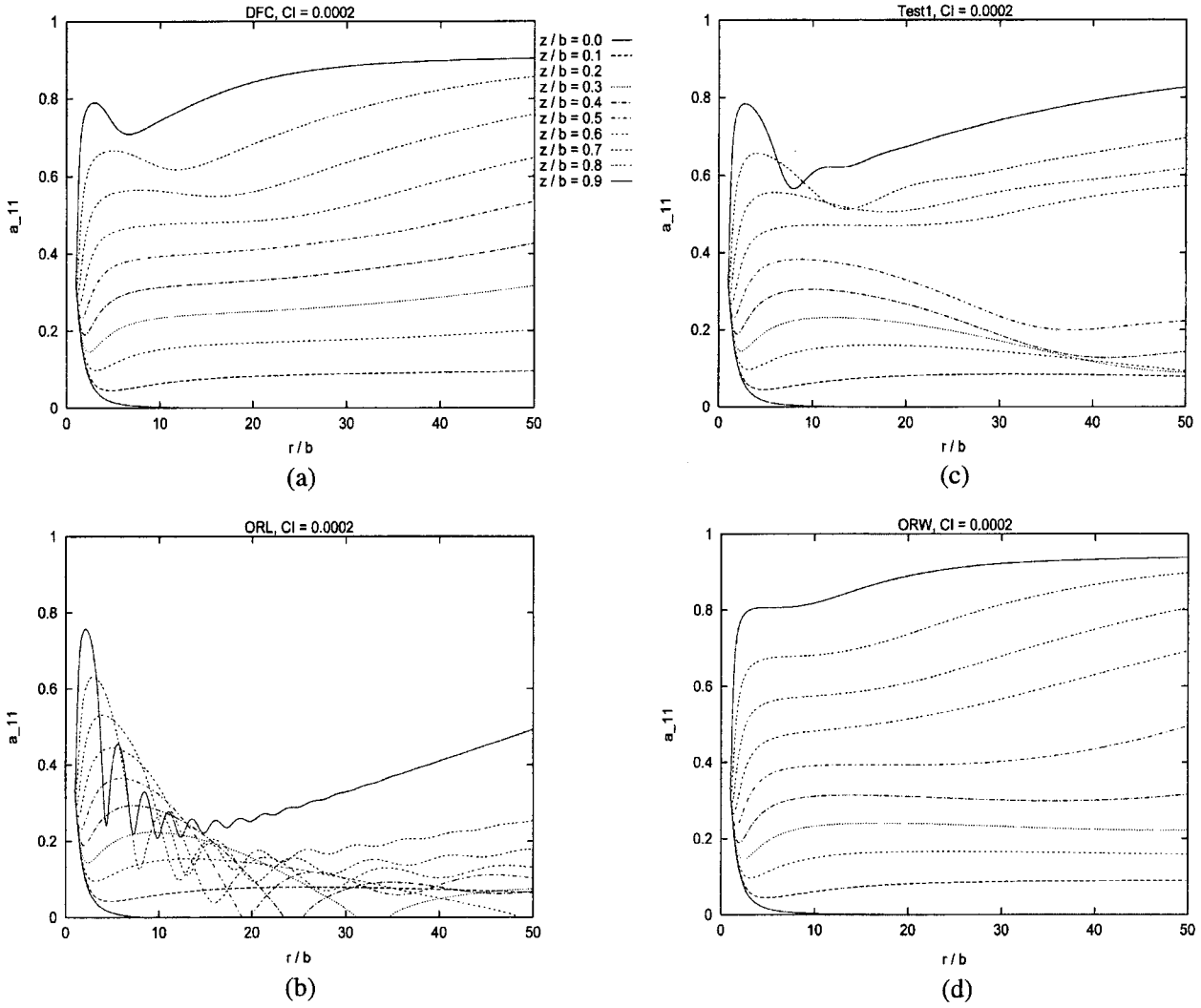

Fig. 5. a_{11} component in isothermal Newtonian radial diverging flow as a function of radial location (r/b) at several thickness positions (z/b) for various closure approximations with C_I=0.0002: (a) DFC, (b) ORL, (c) 'Test1' and (d) ORW.

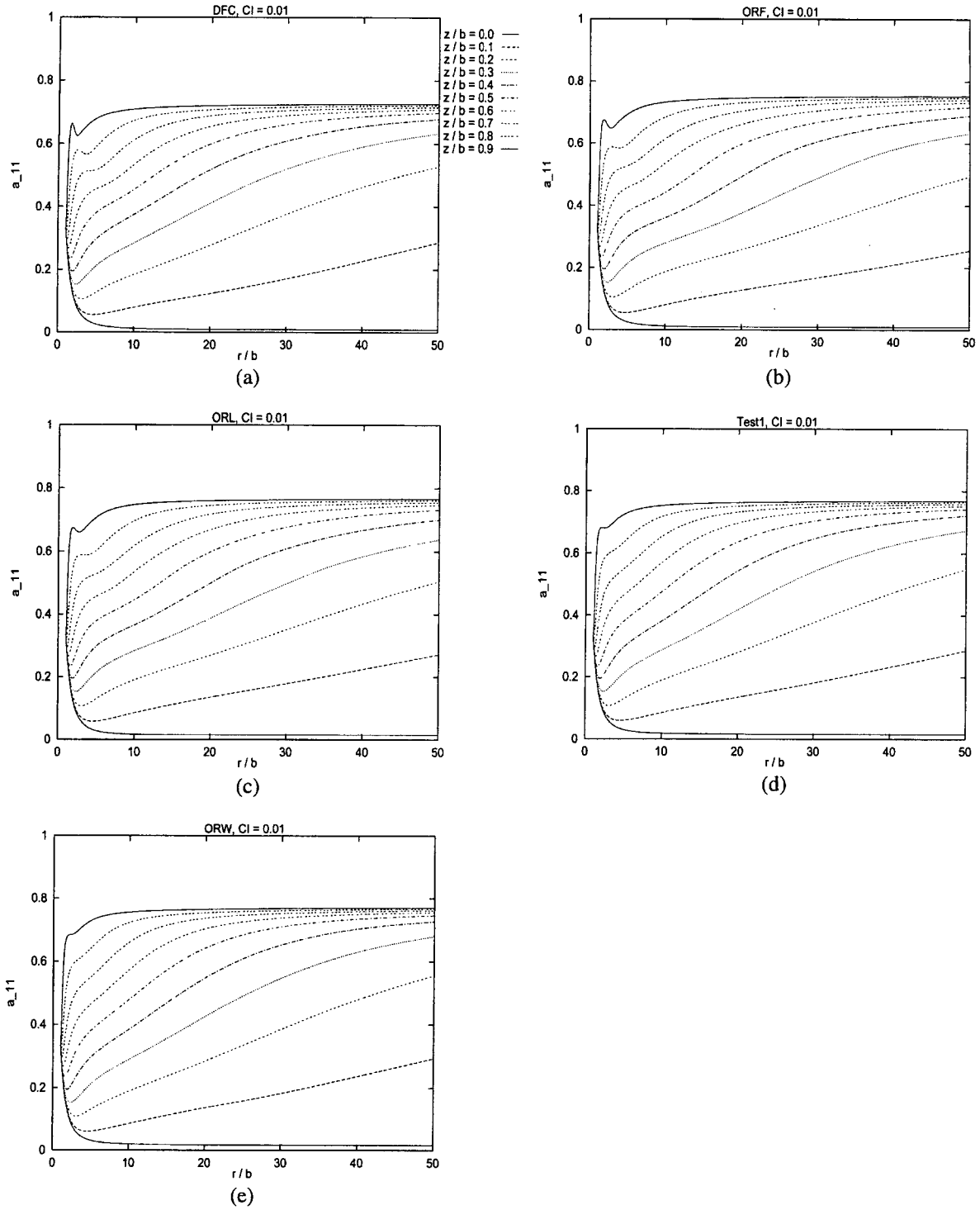

Fig. 6. a_{11} component in isothermal Newtonian radial diverging flow as a function of radial location (r/b) at several thickness positions (z/b) for various closure approximations with C_I=0.01: (a) DFC, (b) ORF, (c) ORL, (d) 'Test1' and (e) ORW.

0001. This is also true for homogeneous flow cases. As shown in Fig. 7 in simple shear flow, ORW does behave very well over a wide range of C_I values. Also in shear/stretch balanced flow, as shown in Fig. 8, ORW behaves best. For other homogeneous flow fields such as uniaxial elongation, biaxial elongation etc, we could find no difference between DFC, ORF, ORL, 'Test 1' and ORW. So in this paper we do not report on these cases.

With such extensive performance evaluations of various closure approximations via the isothermal Newtonian radial

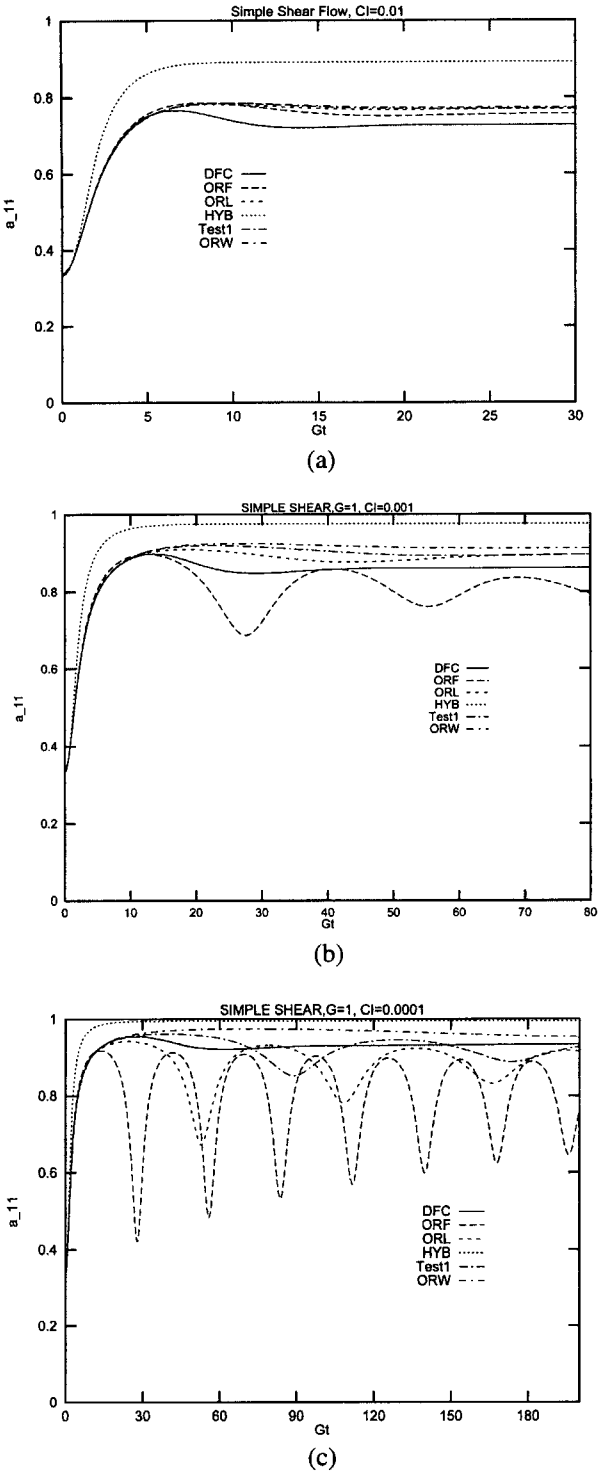

Fig. 7. a_{11} component in simple shear flow (G=1) with comparisons of DFC, ORF, ORL, HYB, Test1 and ORW for (a) C_I=0.01, (b) C_I=0.001 and (c) C_I=0.0001.

diverging flow as well as several homogeneous flows, ORW seems to be our best choice up to the present date.

3.2. Comparisons of Closure Approximations with Experimental Data(Coupled Analysis of Injection Mold Filling Process)

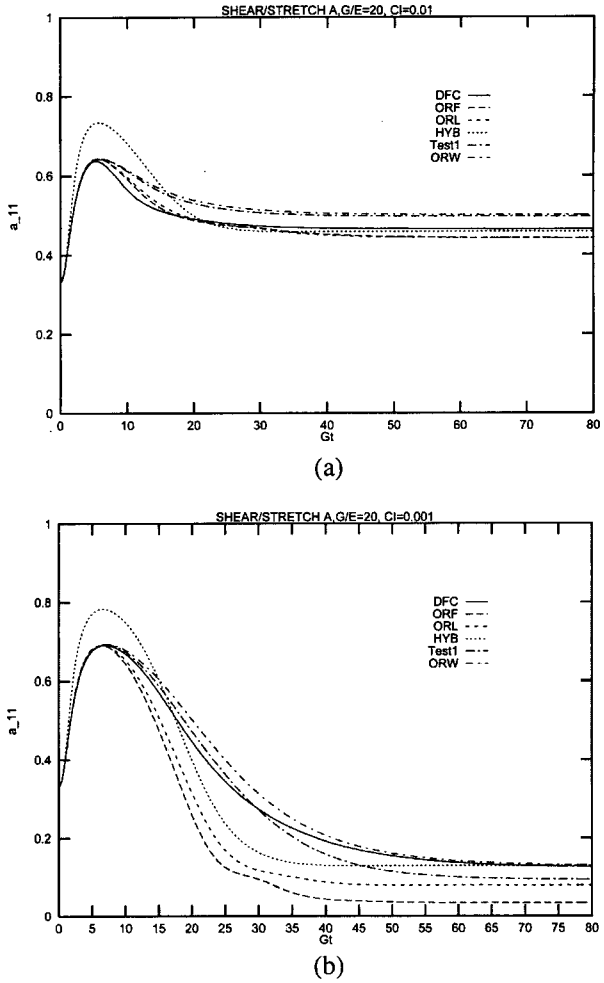

Fig. 8. a_{11} component in shear/stretch A (G/E=20) with comparisons of DFC, ORF, ORL, HYB, Test1 and ORW for (a) C_I=0.01 and (b) C_I=0.001.

We performed coupled analysis of injection mold filling process including in-plane velocity gradient effects for a film-gated strip and a center-gated disk and compared with experimental measurements of fiber orientation of nylon 6/6 reinforced with 43 wt%(v_f=0.23) of glass fibers(Du Pont: Zytel 101L)[8]. The average fiber length L=210 μm and the diameter D=11 μm. The thermal properties and melt viscosity constants for the modified Cross model(Eq. (9)) are shown in Table 1. Finite element meshes used for numerical analysis are shown in Fig. 9 and Fig. 10. Cavity geometry data for the film-gated strip: l=203.2 mm, width W=25.4 mm, and a thickness 2b=3.18 mm. The other cavity geometry data for the center-gated disk: outer radius R_0=76.2 mm and a thickness 2b=3.18 mm. Particle number of N=40.3 is used for simulation based on Dinh and Armstrong's

Table 1. Material properties and viscosity constants of nylon 6/6

Thermal properties (Du Pont: Zytel 70G43L)	
ρ	1.33×10^{3} kg/m^{3}
C_p	1.97×10^{3} J/(kg · K)
k	2.60×10^{-1} W/(m · K)
Viscosity constants for Cross Model (Du Pont: Zytel 70G43L)	
m	0.549
B	4.37×10^{-9} Pa · s
T_b	1.68×10^{4} K
τ^*	3.04×10^{4} Pa

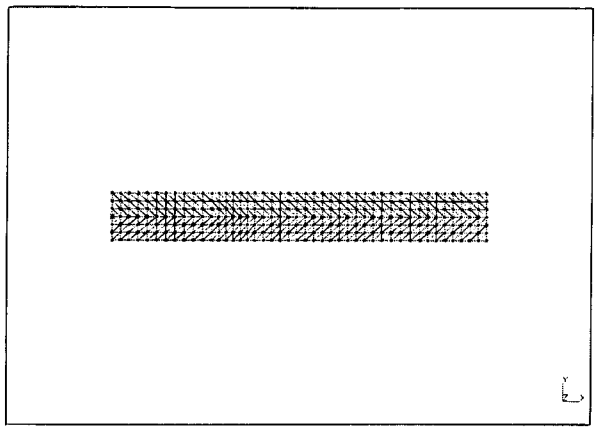

Fig. 9. Finite element mesh for rectangular film-gated strip with 528 elements and 315 nodes.

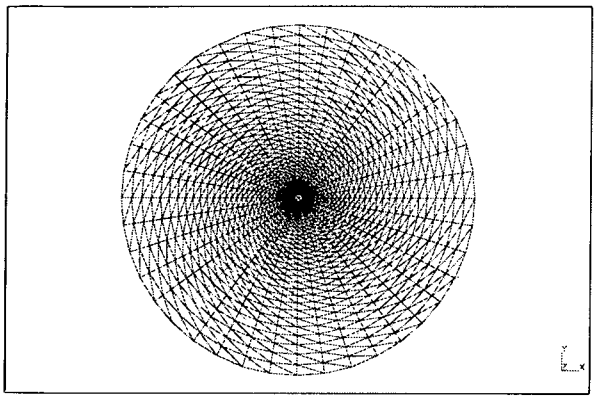

Fig. 10. Finite element mesh for a center-gated-disk with 2400 elements and 1240 Nodes.

theory with Eqs. (5)~(7). For the rectangular strip the process variables were: inlet temperature T_{inlet}=550 K, mold wall temperature T_{wall}=297 K, and the filling time t_{fill}=0.4 s. For the disk the process variables were: T_{inlet}= 550 K, T_{wall}=347 K, t_{fill}=2.5 s.

Shown in Fig. 11 are flow directional orientation component(a_{11}) across the thickness at several flow directional locations(x/b) for a film-gated strip. To compare

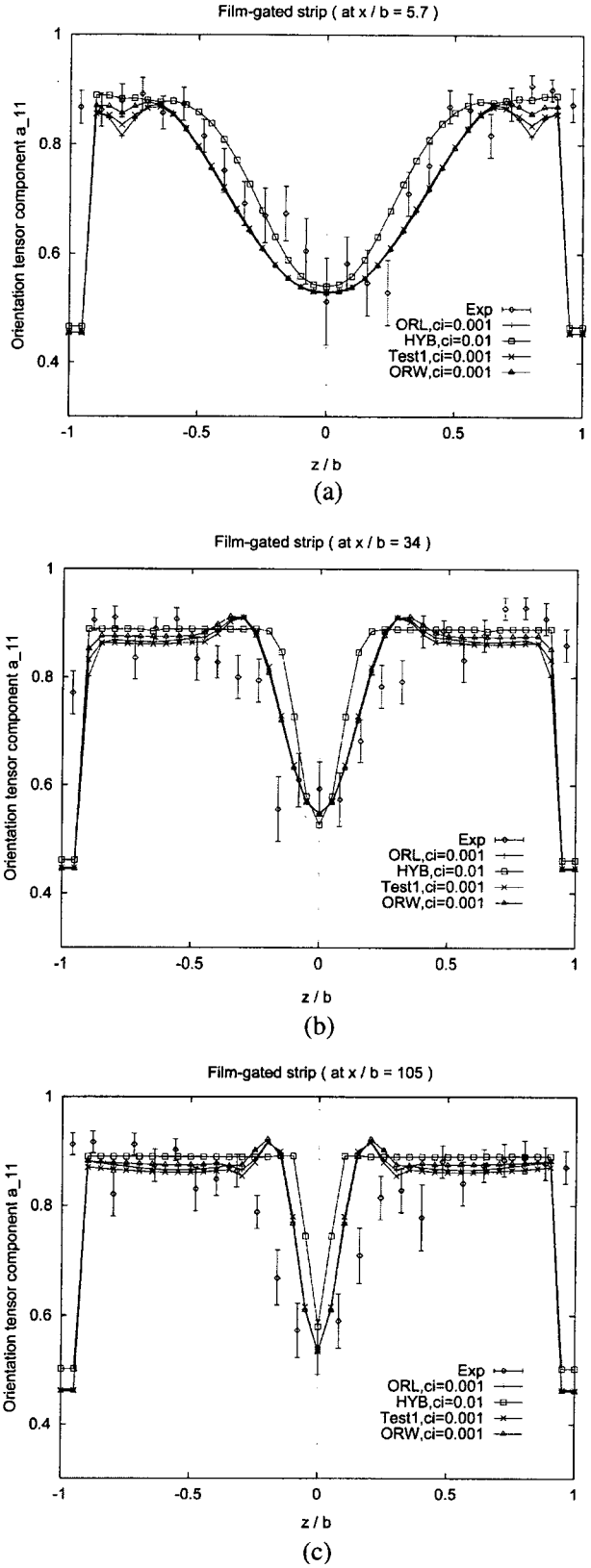

Fig. 11. a_{11} component as a function of thickness positions (z/b) for various closure approximations of ORL, HYB, Test1 and ORW with experimental data for film-gated strip at (a) x/b= 5.7, (b) x/b=34 and (c) x/b=105.

results obtained from various closure approximations with experimental data, C_I=0.001 is used for ORL, 'Test 1' and ORW while C_I=0.01 is used for HYB since results from HYB with C_I=0.001 is too bad to compare. All of them seem to predict a_{11} qualitatively well compared with experimental data. However, all of them show a little over-prediction of flow directional orientation component at far down-stream, resulting in a thinner core than the experimental data. This point is to be further discussed in conjuction with the center-gated disk case as below.

Shown in Fig. 12 are flow directional orientation component(a_{11}) across the thickness at several flow directional locations(r/b) for a center-gated disk. In this comparison, the same values of C_I were used as in the film-gated strip described above. It is important to note that ORL at first glance seems to match with experimental data better than other closure approximations. But as we have seen at the previous section(Fig. 3d) this seemingly better agreement is just a coincidence caused by its under-prediction of flow directional orientation component during its oscillatory behavior compared with DFC. This fact is clearly demonstrated by Fig. 13 which shows as a function of radial location(r/b) at several thickness positions(z/b) in cases of ORL and 'Test1'. As indicated in Fig. 12, 'Test1' and ORW cases show an excellent agreement with experimental data for the range of radial location between the inner radius and about half the radius of the disk. There is not so much difference between 'Test1' and ORW around core and shell layers, but one can observe a little difference at transition layer. As we have seen at the previous section(Fig. 4), ORW matches better with DFC at transition layer than 'Test1'. Therefore, it seems that ORW provides better behavior compared with 'Test1'.

However, as fiber orientation reaches a steady-state, an over-prediction of flow directional orientation component at core layer(i.e., resulting in too thin core layer) is observed as in the case of film-gated strip. Assuming that the experimental data are correct, one may consider the following points to account for such a consistent deviation between the numerical prediction and experimental data.

① Compressibility effect by packing stage may affect orientation behaviors, but by intuition, additional velocity components induced by compressibility will further align flow directional orientation component and thus make thinner core layer. Therefore, incorporating the compressibility effect may not be the right direction to remedy this kind of deviation.

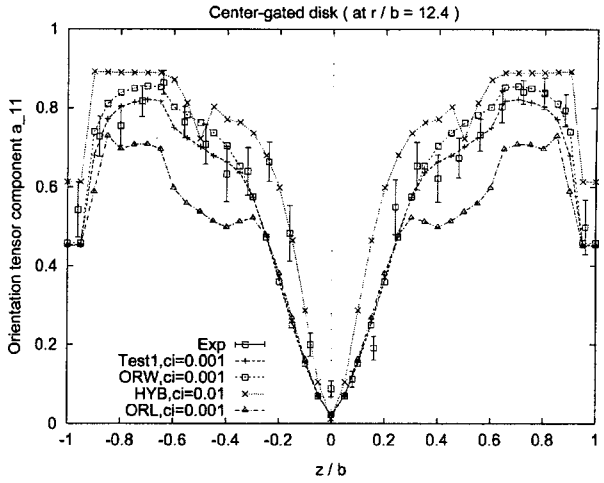

(a)

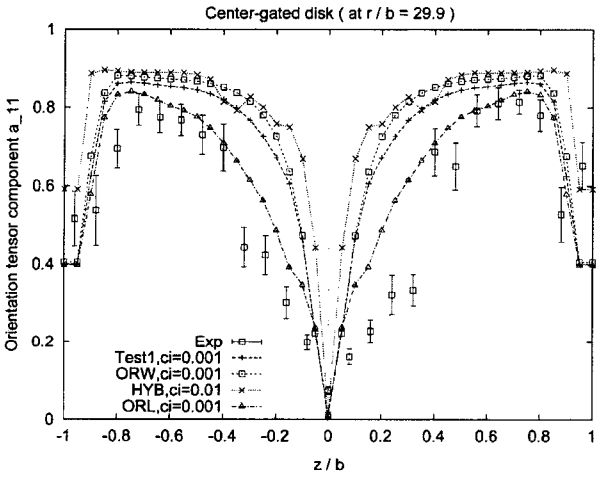

(b)

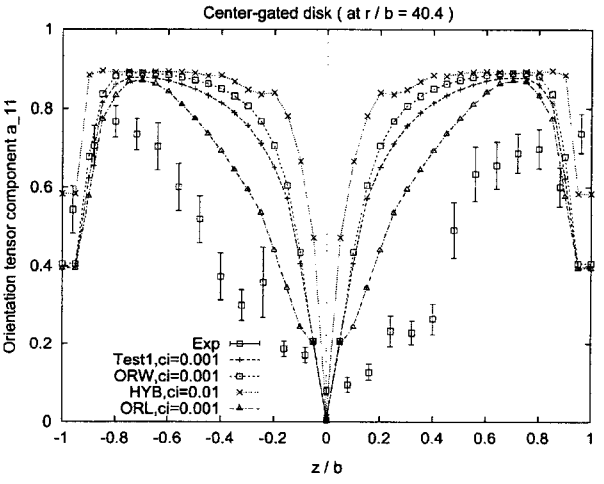

(c)

Fig. 12. a_{11} component as a function of thickness positions (z/b) for various closure approximations of ORL, HYB, Test1 and ORW with experimental data for center-gated disk at (a) r/b =12.4, (b) r/b=29.9 and (c) r/b=40.4.

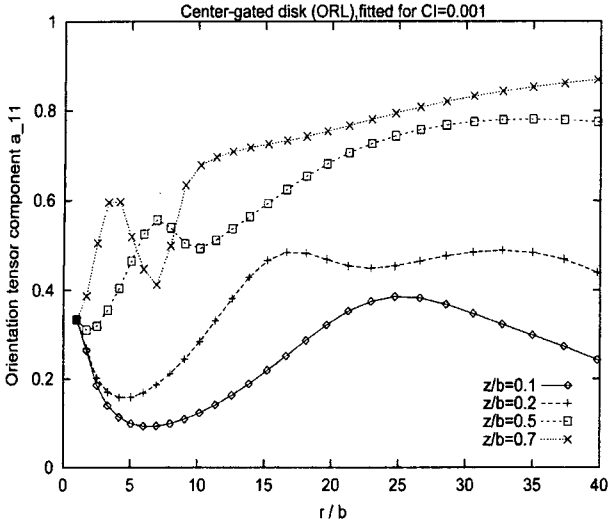

(a)

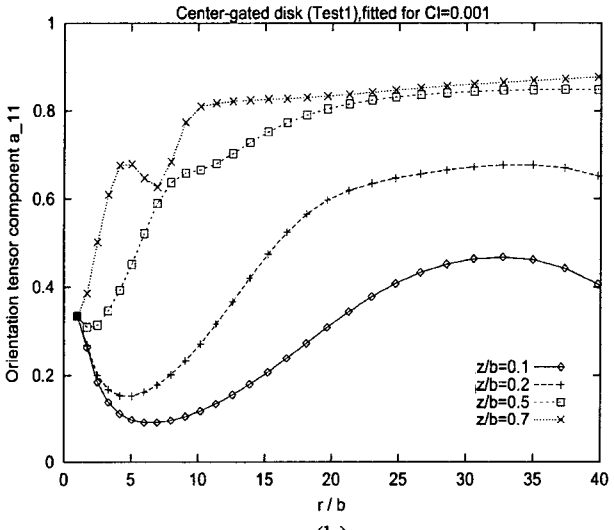

(b)

Fig. 13. Plot of a_{11} vs. r/b for center-gated disk with C_I=0.001 (a) ORL and (b) 'Test1'.

② Diverging effect by thermal boundary layer at wall region induced from large filling time at center-gated disk may reduce the flow directional orientation component around core layers as a kind of randomization effect. This phenomenon is observed as shown in Fig. 13b. A strip with negligible thermal boundary layer due to a short filling time also shows thin core. So the diverging effect should be studied further.

③ Modification of Folgar and Tucker's model for diffusivity term(more specifically, interaction coefficient C_I in $D_r=C_I\dot{\gamma}$[6]) which accounts for fiber-fiber interaction might be necessary. According to this model, the orientation is known to reach the steady-state rather quickly than the experimental data[6]. It seems natural to conceive that the

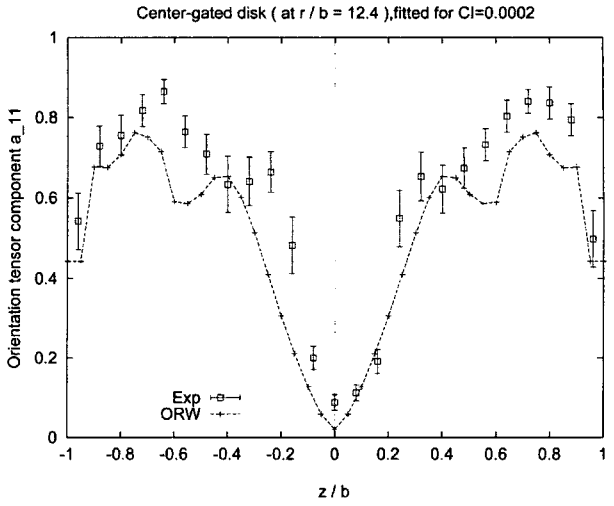

(a)

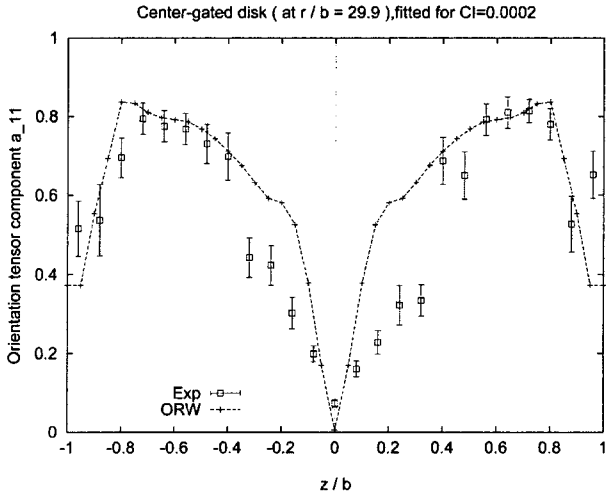

(b)

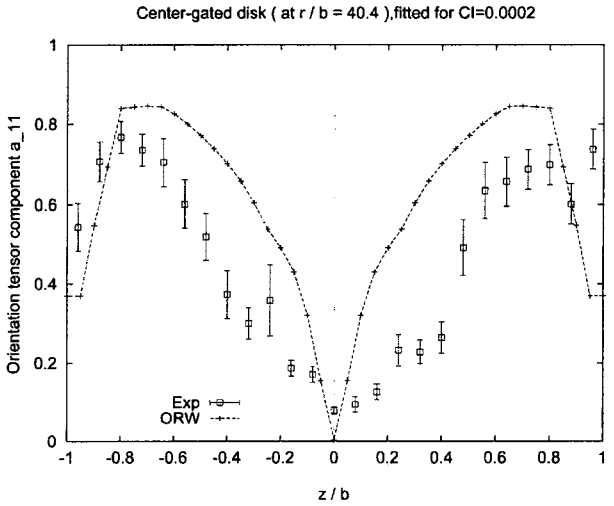

(c)

Fig. 14. Plot of a_{11} vs. z/b for center-gated disk for ORW with C_I= 0.0002 at (a) r/b=12.4, (b) r/b=29.9 and (c) r/b=40.4.

magnitude of interaction is different between the orientation states of transient and steady periods. By intuition, C_I for transient state must be larger than that of steady state. This argument has been discussed in many literatures[6,19-23]. Also, we can verify this argument by performing coupled simulation for center-gated disk for C_I=0.0002 with ORW which are shown in Fig. 14. At far downstream of r/b=40.4, predicted orientation component matches with experimental data better than that for C_I=0.001(Fig. 12c). On the other hand, near the gate(at r/b=12.4) the predicted a_{11} with C_I=0.001 is closer to experimental data than that with C_I=0.0002. In summary, it looks plausible that near gate where orientation state is still transient, C_I=0.001 is appropriate and at far downstream where steady orientation state is reached, $C_I \leq 0.0002$ is more appropriate. More study is in order along this line.

4. Concluding Remarks

We have extensively performed numerical evaluation of various closure approximations with several homogeneous flows, radial diverging flow field and with real injection molding experimental cases of a film-gated strip and a center-gated disk. It is well known that the generally used Hybrid closure approximation over-predicts flow directional orientation components a_{11}. It was found that ORF and ORL, previous Orthotropic closure approximations suffer from non-physical oscillations in radial diverging flows for low values of interaction coefficient C_I.

As an effort to eliminate such a non-physical oscillation, we have successfully introduced 'Test1' and ORW which are improved versions of previous Orthotropic closure approximation. Both 'Test1' and ORW have overcome the critical defect(non-physical oscillatory behavior) which ORF and ORL suffer from. Between 'Test1' and ORW, ORW seems to be capable of predicting fiber orientation behavior better for all the homogeneous flow fields and non-homogeneous flow fields over a wider range of C_I value, i.e., $C_I > 0.0001$. In this regard, ORW seems to be our best choice since it is in excellent agreement with DFC for various flow fields. Thus the goal of having a good closure approximation is likely to have been achieved successfully by ORW.

However, deviations between the predicted results from ORW and experimental data still exist in both the film-gated strip and the center-gated disk cases as indicated in Fig.11 and 12. This kind of deviation cannot be removed by other closure approximation unless one modifies the governing equation of fiber distribution function in terms of the diffusivity term which accounts for fiber-fiber interaction. If the experimental data in the literature are correct, it may be crucial to modify the diffusivity term based on hydrodynamic theory to achieve a further improvement in the physical modellings of fiber orientation. Diffusivity term can be divided into two parts: one is interaction coefficient C_I which models magnitude of fiber-fiber interaction and the other is generalized shear rate $\dot{\gamma}$ which models frequency of fiber-fiber interaction. If we assume that steady-state orientations of homogeneous flows do not depend upon $\dot{\gamma}$, $\dot{\gamma}$ must be linear in the evolution equation of Eq. (3). This is supported by experimental data of Bibbo and Armstrong[24]. So only C_I remains to be modified. However, there were also contradictory experimental results of Kamal and Mutel[25] that predict different steady state orientations for different shear rates. If this is indeed the case, a modification of $\dot{\gamma}$ might also have to be considered. Many researchers have indicated and argued that C_I must be a function of orientation states. N. Phan Thien et al.[23] argued that diffusivity must be anisotropic, so tensorial form should be introduced. But it is not so easy to extract a general model of anisotropic tensorial diffusivity. Further study is in order along this line of thought.

Appendix

New coefficients of ORW are as follows:

$$\begin{Bmatrix} \bar{A}_{11} \\ \bar{A}_{22} \\ \bar{A}_{33} \\ \bar{A}_{44} \\ \bar{A}_{55} \\ \bar{A}_{66} \end{Bmatrix} = \begin{bmatrix} 0.070055 & 0.339376 & 0.590331 \\ 0.115177 & -0.368267 & 0.252880 \\ 1.249811 & -2.148297 & 0.898521 \\ -0.125192 & 0.383588 & -0.258401 \\ -0.110411 & 0.736232 & -0.625796 \\ 0.011340 & -0.017855 & 0.006730 \end{bmatrix} \begin{bmatrix} -0.396796 & 0.333693 & 0.411944 \\ 0.094820 & 0.800181 & 0.535224 \\ -2.290157 & 1.044147 & 1.934914 \\ 0.836820 & -0.714844 & -0.966729 \\ 0.413924 & -0.303888 & -0.928577 \\ 0.064527 & -0.082800 & 0.435217 \end{bmatrix} \times \begin{Bmatrix} 1 \\ a_1 \\ a_1^2 \\ a_2 \\ a_2^2 \\ a_1 a_2 \end{Bmatrix}$$

Nomenclature

a_{ij} : Second-order orientation tensor.

a_{ijkl} : Fourth-order orientation tensor.

$\hat{a}_{ijkl}$: Linear closure approximation for fourth-order

orientation tensor.

$\tilde{a}_{ijkl}$: Quadratic closure approximation for fourth-order orientation tensor.

$\bar{a}_{ijkl}$: Hybrid closure approximation for fourth-order orientation tensor.

a_1, a_2, a_3: Eigenvalues of second-order orientaton tensor in descending order in magnitude.

$\bar{A}_{mm}$: Principal values of fourth-order orientation tensor.

a_c : Actual average interfiber spacing.

b : Half gap thickness.

C_I : Interaction coefficient for fiber orientation.

C_p : Thermal capacity of the thermoplastic medium.

D : Fiber diameter.

E : elongation rate for elongational flow.

D_r : Diffusivity term which accounts for fiber-fiber interaction.

f : Scalar measure of orientation.

G : shear rate for simple shear flow.

h : Average distance from a given fiber to its nearest neighbor.

K : A univeral constant of proportionality.

k : Thermal conductivity of the thermoplastic medium.

l : Chracteristic length of injection molded part.

L : Fiber length.

n : Number of fibers per unit volume.

n_x, n_y : Components of unit outward normal vector on the boundary.

N : Particle number.

p : Fiber unit direction.

$\dot{p}_i$: Fiber angular velocity.

P : Pressure.

Q : Inlet volume flow rate.

R_0 : Outer radius of center-gatd-disk.

t : Time variable.

t_{full} : Filling time.

T : Temperature.

T_{inlet} : Inlet melt temperature.

T_{wall} : Mold wall temperature.

u, v : In-plane velocity components with respect to local coordinate.

$\bar{u}, \bar{v}$: Gapwise average velocity.

u_r, u_θ, u_z: Velocity components in cylindrical coordinate system.

$u_{i,j}$: $\partial u_i/\partial x_j$, velocity gradient tensor.

v_f : Volume fraction of fibers.

W : width of injection molded part.

w : Gapwise velocity components with respect to local coordinate.

x, y, z : Local coordinate system.

r, θ, z : Local cylindrical coordinate system.

m, B, C, T_b : Coefficients of viscosity function.

D/Dt : Material derivative.

II, III : Second and third principal invariants of a_{ij}

Greek letters

ψ : Probability distribution function.

$\dot{\gamma}$: Generalized shear rate.

$\dot{\gamma}_{ij}$: Rate of deformation tensor.

δ_{ij} : Unit tensor.

η : Viscosity of the thermoplastic medium.

η_0 : Zero shear rate viscosity.

λ : Geometric parameter related to the particle aspect ratio.

ρ : Density of the thermoplastic medium.

τ_{ij} : Stress tensor.

ω_{ij} : Vorticity tensor.

χ^2 : Merit function value to minimize.

References

1. J.C. Halpin and J.L. Kardos, The Halpin-Tsai Equations: A Review, *Polym. Eng. Sci.*, **16**, 344 (1976).
2. S.T. Chung and T.H. Kwon, *Polym. Eng. Sci.*, **35**, 604 (1995).
3. S.T. Chung and T.H. Kwon, *Polym. Compos.*, **17**, 859 (1996).
4. S.M. Dinh and R.C. Armstrong, *J. Rheol.*, **28**, 207 (1984).
5. G.B. Jeffery, *Proc. R. Soc.*, **A102**, 161 (1922).
6. F. Folgar and C.L. Tucker, *J. Reinf. Plast. Compos.*, **3**, 98 (1984).
7. S.G. Advani and C.L. TuckerIII, *J. Rheol.*, **31**, 751 (1987).
8. R.S. Bay and C.L. TuckerIII, *Polym. Compos.*, **13**, 332 (1992).
9. G.L. Hand, *J. Fluid. Mech.*, **13**, 33 (1962).
10. G.G. Lipscomb, M.M. Denn, D.U. Hur and D. Boger, *J. Non-Newtonian Fluid Mech.* **26**, 297 (1988).
11. M. Doi, *J. Polym. Sci., Polym. Phys. Ed.* **19**, 229 (1981).
12. G. Marrucci and N. Grizzuti, *J. Non-Newtonian Fluid Mech.* **14**, 103 (1984).
13. E.J. Hinch and L.G. Leal, *J. Fluid Mech.* **76**, 187 (1976).
14. S.G. Advani and C.L. TuckerIII, *J. Rheol.*, **34**, 367 (1990).
15. Verleye, V. and F. Dupret, *Proc. of the ASME Winter Annual Mtg.* MD-Vol49. HTD-Vol283, 1994, p. 265.
16. J.S. Cintra, Jr. and C.L. TuckerIII, *J. Rheol.*, **39**, 1095 (1995).
17. G.K. Batchelor, *J. Fluid Mech.*, **46**, 813 (1971).
18. C.L. Tucker, *J. Non-Newtonian Fluid Mech.*, **39**, 239 (1991).
19. 12. C.A. Stover and Cohen, *J. Fluid Mech.*, **238**, 277 (1992).
20. S.G. Shaqfeh and D.L. Koch, *Phys. Fluids*, **31**(4), 728 (1988).
21. S.G. Shaqfeh and D.L. Koch, *Phys. Fluids A*, **2**(7), 1077 (1990).
22. P.L. Frattini *et al.*, *Phys Fluids A*, **3**(11), 2516 (1991).
23. X.J. Fan and N. Phan-Thien, *J. Non-Newtonian Fluid Mech.*, **74**, 113 (1998).
24. Bibbo, M.A. and R.C. Armstrong, *The Manufacturing Science of Composites*, **4**, 105 (1988).
25. Mutel, A.T. and M.R. Kamal, *SPE ANTEC Proc.* 1987, p. 732.